CKA-EUTERPE and SCENIC for W7-X

C. Slaby[1], A. Könies[1], R. Kleiber[1], M. Machielsen[2], J. Graves[2], S. Lazerson[1]

[1] Max Planck Institute for Plasma Physics, Wendelsteinstraße 1, 17491 Greifswald, Germany
[2] Ecole Polytechnique Fédérale de Lausanne (EPFL), Swiss Plasma Center (SPC), CH-1015 Lausanne, Switzerland

May 30, 2022

This work has been carried out within the framework of the EUROfusion Consortium, funded by the European Union via the Euratom Research and Training Programme (Grant Agreement No 101052200 — EUROfusion). Views and opinions expressed are however those of the author(s) only and do not necessarily reflect those of the European Union or the European Commission. Neither the European Union nor the European Commission can be held responsible for them.

Contents

Contents

shear Alfvén continuum

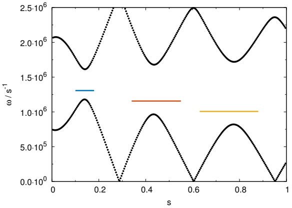

- CKA (ideal MHD) provides the modes / EUTERPE calculates the fast-particle power transfer
- here: single CKA simulation with phase factor $e^{\mathrm{i}[m_0\vartheta+n_0\varphi]}$ $(m_0 = 11, n_0 = -6)$ (identical for all modes)
- does not represent the typical stellarator case well
- usually modes from different CKA runs, with different phase factors, need to be combined

radial mode structures

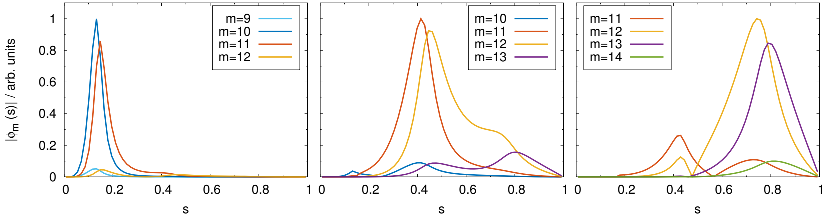

The new multi-mode model I (CKA example)

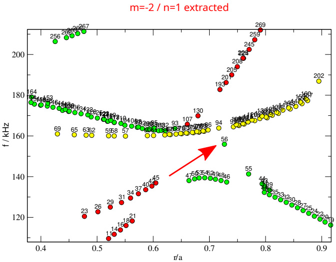

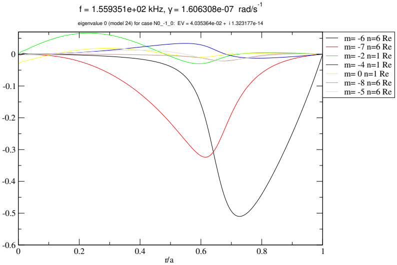

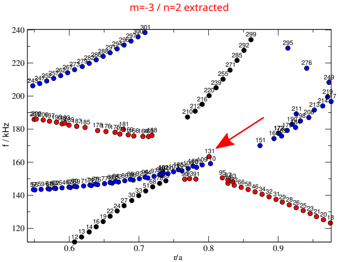

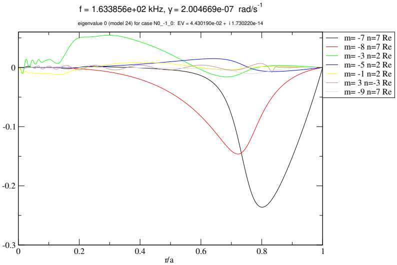

The new multi-mode model II

Old multi-mode model

- all modes come from a single CKA calculation
- all modes have the same phase factor
- phase factor in EUTERPE set by CKA

New multi-mode model

- several CKA calculations can be combined
- modes with any phase factor can be combined
- phase factor is no longer extracted in EUTERPE (always full potential)

The new multi-mode model II

Old multi-mode model

- all modes come from a single CKA calculation
- all modes have the same phase factor
- phase factor in EUTERPE set by CKA

New multi-mode model

- several CKA calculations can be combined
- modes with any phase factor can be combined
- phase factor is no longer extracted in EUTERPE (always full potential)

- this change is in principle trivial, but phase-factor extraction goes very deep in EUTERPE
- numerous places needed to be changed (was quite a bit of work)
- new version has been benchmarked and is ready for use now
- currently being employed for some experimental cases / no results to show yet

CKA-EUTERPE is based on the gyrokinetic density equation

$$\frac{\partial}{\partial t}\nabla\cdot\left[\frac{m_\mathrm{i}n_\mathrm{i}}{B^2}\nabla_\perp\phi\right] = \nabla\cdot\left\{j_\|^{(1)}\mathbf{b} + j_\|^{(0)}\left[\frac{\mathbf{b}\times\boldsymbol{\kappa}}{B}A_\| - \frac{\mathbf{b}\times\nabla A_\|}{B}\right] + \right.$$
$$+ p_\|^{(1)}\frac{\mathbf{b}\times\boldsymbol{\kappa}}{B} + p_\perp^{(1)}\frac{\mathbf{b}\times\nabla B}{B^2} + \qquad (1)$$
$$\left. + p_{\|,\mathrm{fast}}^{(1)}\frac{\mathbf{b}\times\boldsymbol{\kappa}}{B} + p_{\perp,\mathrm{fast}}^{(1)}\frac{\mathbf{b}\times\nabla B}{B^2}\right\}$$

as well as Ampère's law

$$-\nabla_\perp^2 A_\| = \mu_0 j_\|^{(1)}, \qquad (2)$$

and Ohm's law

$$-\frac{\partial}{\partial t}A_\| - \mathbf{b}\cdot\nabla\phi = -\frac{\mathbf{b}\cdot\nabla}{en_{0,\mathrm{e}}}p_{\|,\mathrm{e}}^{(1)}. \qquad (3)$$

We make a complex mode ansatz for ϕ and $A_\|$

$$\phi(\mathbf{r},t) = \frac{1}{2}\sum_j\left[\hat{\phi}_j(t)\,\phi_{0,j}(\mathbf{r})\exp(\mathrm{i}\omega_j t) + \hat{\phi}_j^*(t)\,\phi_{0,j}^*(\mathbf{r})\exp(-\mathrm{i}\omega_j t)\right] \qquad (4)$$

$$A_\|(\mathbf{r},t) = \frac{1}{2}\sum_j\left[\hat{A}_j(t)\,A_{0,j}(\mathbf{r})\exp(\mathrm{i}\omega_j t) + \hat{A}_j^*(t)\,A_{0,j}^*(\mathbf{r})\exp(-\mathrm{i}\omega_j t)\right] \qquad (5)$$

Insert ansatz into Ohm's law and multiply resulting equation with

$$-\nabla_\perp^2 \left[\hat{A}_k^* A_{0,k}^* (\mathbf{r}) \exp(-\mathrm{i}\omega_k t)\right] \tag{6}$$

and drop all terms proportional to $\exp[-\mathrm{i}(\omega_j + \omega_k) t]$ (fast oscillations). This yields the first amplitude equation

$$\frac{\partial}{\partial t}\hat{A}_j + \mathrm{i}\omega_j \left(\hat{A}_j - \hat{\phi}_j\right) = \sum_k \hat{\mathbb{N}}_{jk}^{-1} u_k \hat{A}_j. \tag{7}$$

where

$$\hat{\mathbb{N}}_{jk} = \hat{A}_j \hat{A}_k^* \exp[\mathrm{i}(\omega_j - \omega_k) t] \int \mathrm{d}^3\mathbf{r} \nabla_\perp A_{0,j} \cdot \nabla_\perp A_{0,k}^* \tag{8}$$

and

$$u_k = -2\mu_0 \int \mathrm{d}^3\mathbf{r} \left[\frac{\mathbf{B}\cdot\nabla B}{-B^2} j_{\parallel 0}^{(1)*} + \mathbf{b}\cdot\nabla\left(j_{\parallel 0}^{(1)*}\right)\right] \frac{\hat{A}_k^* \exp(-\mathrm{i}\omega_k t)}{e n_{0,\mathrm{e}}} \times \\ \times \int \mathrm{d}\mu \mathrm{d}v_\parallel \mathrm{d}\alpha B_\parallel^\star m_\mathrm{e} v_\parallel^2 f_\mathrm{e}^{(1)} \tag{9}$$

For the second equation we insert the ansatz into the time derivative of the gyrokinetic density equation, perform a multiplication with

$$\hat{\phi}_k^* \phi_{0,k}^* (\mathbf{r}) \exp(-\mathrm{i}\omega_k t) \tag{10}$$

and again neglect terms proportional to $\exp[-\mathrm{i}(\omega_j + \omega_k) t]$. This yields the second amplitude equation

$$\frac{\partial}{\partial t}\hat{\phi}_j + \mathrm{i}\omega_j \left(\hat{\phi}_j - \hat{A}_j\right) = -\sum_k \hat{\mathbb{M}}_{jk}^{-1} T_k \hat{\phi}_j \tag{11}$$

where

$$\hat{\mathbb{M}}_{jk} = \frac{1}{2}\hat{\phi}_j \hat{\phi}_k^* \exp[\mathrm{i}(\omega_j - \omega_k) t] \int \mathrm{d}^3\mathbf{r}\, \frac{m_\mathrm{i} n_\mathrm{i}}{B^2} \nabla_\perp \phi_{0,j} \cdot \nabla_\perp \phi_{0,k}^*. \tag{12}$$

and

$$T_k = \int \mathrm{d}^3\mathbf{r} \int \mathrm{d}\mu \mathrm{d}v_\parallel \mathrm{d}\alpha B_\parallel^\star \left\{ \frac{\mathbf{b}\times}{Z\mathrm{e}} \left(\frac{m_\mathrm{f} v_\parallel^2}{B}\boldsymbol{\kappa} + \frac{\mu}{B}\nabla B \right) \cdot \right. \\ \left. \cdot \left(-Z\mathrm{e}\nabla\phi_{0,k}^* \hat{\phi}_k^* \exp(-\mathrm{i}\omega_k t)\, f_\mathrm{fast}^{(1)} \right) \right\}. \tag{13}$$

Case description

- standard ITPA case, but with twice the fast-ion density to reach nonlinear saturation earlier

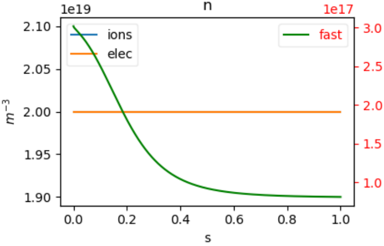

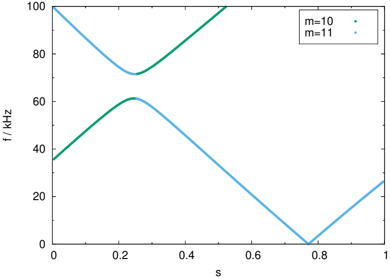

- $m = 10, 11/n = -6$ TAE mode in the gap of the continuum as usual

Results for the ITPA benchmark case

no $E_{||}$

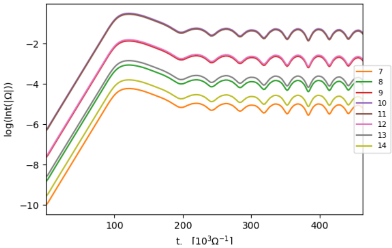

$f = 63.5$ kHz $\quad \gamma = 3.673 \cdot 10^4 \ \mathrm{s}^{-1}$

with $E_{||}$

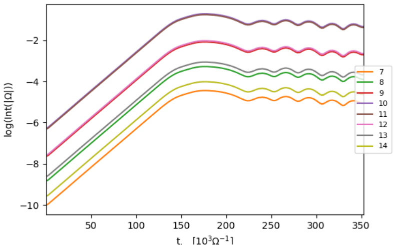

$f = 62.1$ kHz $\quad \gamma = 2.461 \cdot 10^4 \ \mathrm{s}^{-1}$

- linear frequency unchanged when finite $E_{||}$ is included
- linear growth rate reduced by about $1/4$ (trend is expected)
- nonlinear saturation reached later in the simulation
- saturation level comparable (overshoot smaller)
- nonlinear frequency chirping only affected marginally

CKA-EUTERPE uses the $v_\parallel$-formulation of the equations

$$\dot{v}_\parallel = -\mu\nabla B\cdot\left[\mathbf{b}+\frac{m_s}{q_s}\frac{v_\parallel}{BB^\star_\parallel}(\nabla\times\mathbf{B})_\perp\right]-\frac{q_s}{m_s}\frac{\partial\left\langle A_\parallel\right\rangle}{\partial t}$$
$$-\frac{q_s}{m_s}\left\{\mathbf{b}+\frac{m_s}{q_s}\frac{v_\parallel}{BB^\star_\parallel}\left[\mathbf{b}\times\nabla B+(\nabla\times\mathbf{B})_\perp\right]\right\}\cdot\nabla\left\langle\phi\right\rangle \quad (14)$$
$$-\frac{\mu}{B^\star_\parallel}\left[\mathbf{b}\times\nabla B\cdot\nabla\left\langle A_\parallel\right\rangle+\frac{1}{B}\nabla B\cdot(\nabla\times\mathbf{B})_\perp\left\langle A_\parallel\right\rangle\right]$$

$$E_\parallel = -\mathbf{b}\cdot\nabla\phi-\frac{\partial A_\parallel}{\partial t} \quad\longrightarrow\quad -\sum_j A_{0,j}\exp\left(\mathrm{i}\omega_j t\right)\sum_k \hat{\mathbb{N}}^{-1}_{jk}u_k\hat{A}_j \quad (15)$$

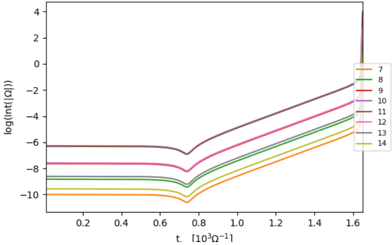

- numerical instability develops instantly
- cannot be mitigated by using smaller time step or larger electron mass
- reason is unclear at the moment

Short summary and next steps

- CKA-EUTERPE model is still extended with new features
  - more general multi-mode version
  - new physics like finite $E_{||}$
- apply the new model to W7-X cases (suitable cases have to be identified)
- goal: can become the basis of a transport model that also works in stellarator geometry, but must be properly benchmarked
- a benchmark with the LIGKA-HAGIS model would be interesting

Contents

- SCENIC[1] is now run in Greifswald to model ICRH physics
- iterative procedure of three (coupled) codes
- usually $5 - 10$ iterations necessary to find consistent solution
  - ANIMEC (anisotropic equilibrium)
  - LEMan (full-wave code / plasma enters with its dielectric tensor)
  - VENUS-LEVIS (particle following in the ICRH wave field / Monte-Carlo kicks)

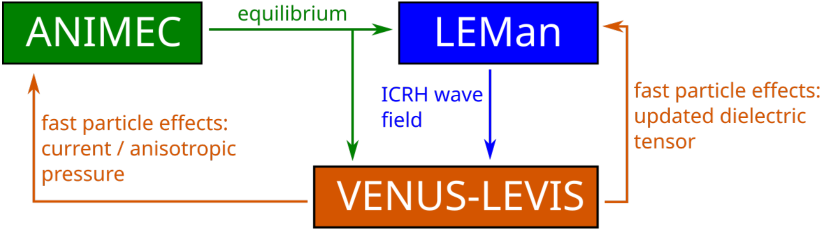

adapted from M. Machielsen

[1] M. Jucker et al., Comm. Phys. Commun. 183, 912-925 (2011)

- LEMan = full wave code that solves Maxwell's equations in potential form

$$\nabla^2 \mathbf{A} + k_0^2 \hat{\epsilon} \cdot \mathbf{A} + \mathrm{i} k_0 \hat{\epsilon} \cdot \nabla \phi = -\frac{4\pi}{c} \mathbf{j}_{\mathrm{ant}} \quad (16)$$

$$\nabla \cdot (\hat{\epsilon} \cdot \nabla \phi) - \mathrm{i} k_0 \nabla \cdot (\hat{\epsilon} \cdot \mathbf{A}) = -4\pi \rho_{\mathrm{ant}} \quad (17)$$

using Coulomb gauge $\nabla \cdot \mathbf{A} = 0$ $\qquad k_0 = \omega / c$

- plasma is included via its dielectric tensor $\hat{\epsilon}$ (different approximations possible: cold / warm / hot plasma)
- code uses finite elements in radial direction and a Fourier expansion in the angular directions

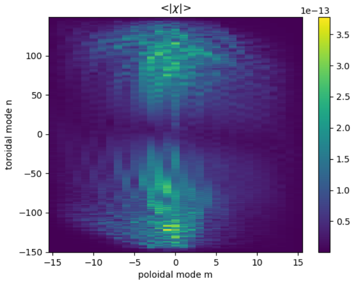

- typically, many poloidal and toroidal modes need to be included to ensure convergence
- no couplings outside a given mode family → separate simulation can be done for each of the 5 mode families and total wave field reconstructed from this data (saves computing resources)

VENUS-LEVIS solves guiding-centre drift-kinetic equations

$$\dot{\mathbf{X}} = v_{\parallel}\frac{\mathbf{B}^{\star}}{B_{\parallel}^{\star}} + \frac{\mathbf{E}^{\star}\times\mathbf{b}}{B_{\parallel}^{\star}} \tag{18}$$

$$\dot{v}_{\parallel} = \frac{q}{m}\frac{\mathbf{B}^{\star}\cdot\mathbf{E}^{\star}}{B_{\parallel}^{\star}} \tag{19}$$

with

$$\mathbf{E}^{\star} = \mathbf{E} - \left(\frac{\mu}{q} + v_{\parallel}\rho_{\parallel}\right)\nabla B - \rho_{\parallel}\dot{\mathbf{B}} \tag{20}$$

$$\mathbf{B}^{\star} = \mathbf{B} + \rho_{\parallel}\nabla\times\mathbf{B} \tag{21}$$

$$B_{\parallel}^{\star} = \mathbf{b}\cdot\mathbf{B}^{\star} \tag{22}$$

quasi-linear operator applies ICRH kicks to the particles (collisions also included)

$$\Delta v_{\perp} = \frac{\left\langle \Delta v_{\perp}^{2}\right\rangle}{2v_{\perp}} + \mathbb{R}\sqrt{2\left\langle \Delta v_{\perp}^{2}\right\rangle} \tag{23}$$

$$\left\langle \Delta v_{\perp}^{2}\right\rangle = \tau^{2}\gamma\frac{Z_{\alpha}^{2}}{m_{\alpha}^{2}}\left|E^{+}e^{-\mathrm{i}\psi}J_{n-1}\left(\frac{k_{\perp}v_{\perp}}{\Omega_c}\right) + E^{-}e^{+\mathrm{i}\psi}J_{n+1}\left(\frac{k_{\perp}v_{\perp}}{\Omega_c}\right)\right|^{2} \tag{24}$$

$$\Delta v_{\parallel} = \frac{k_{\parallel}}{\Omega_c}v_{\perp}\Delta v_{\perp} \tag{25}$$

Equations taken from H. Patten's PhD thesis

- simulations with high Fourier resolution $m \in [-15, 15]$, $n \in [-150, 149]$ have been performed
- split into 5 separate simulations (for the 5 mode families of W7-X $\rightarrow 5 \cdot 1860$ modes)

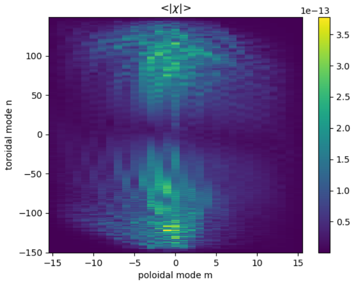

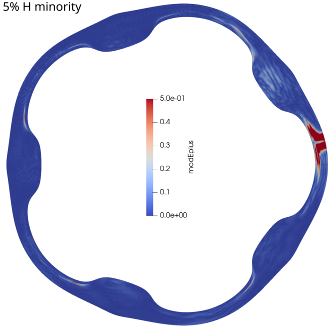

- high resolution needed to resolve small structures $\rightarrow$ realistic results

Aims:

- provide theoretical support for ICRH operation
- first plasmas with ICRH will be He-plasmas with H-minority
- verify that power is indeed absorbed by H-minority (fundamental resonance)

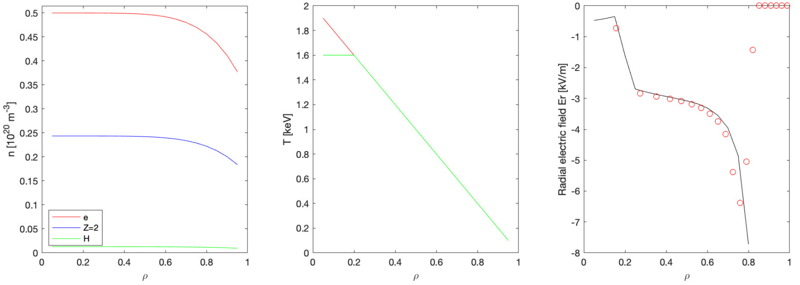

- similar profiles available for 10% and 15% Hydrogen concentration and for higher Helium (bulk plasma) densities
- radial electric field comes from NEOTRANSP

Power absorption depends on H minority concentration

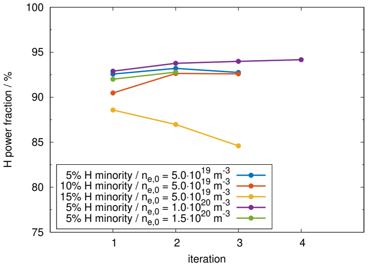

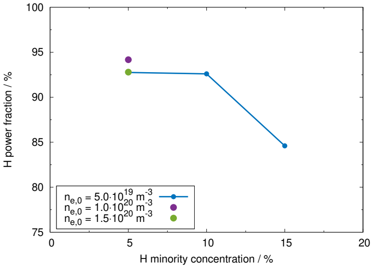

- 3 iterations of SCENIC package performed for each minority concentration
- H power absorption in the range of $\approx 92\%$ for the cases with 5 and 10% H minority (converged)
- H power absorption drops to $\approx 85\%$ for 15% H minority (not converged yet)
- this can hopefully be compared to experimental data in the future

Absorbed power affects formation of FI distribution function

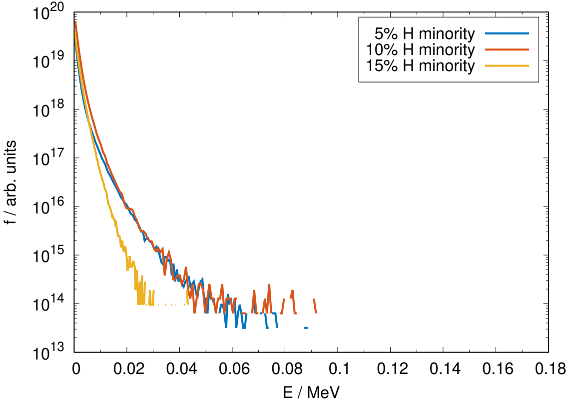

- H minority absorbs least amount of power at 15% concentration

$\Rightarrow$ fewer fast ions

- (standard minority heating scheme is not beneficial for fast-ion generation anyway)

Comparison of the ICRH wave field ($|E_+|$)

5% H minority

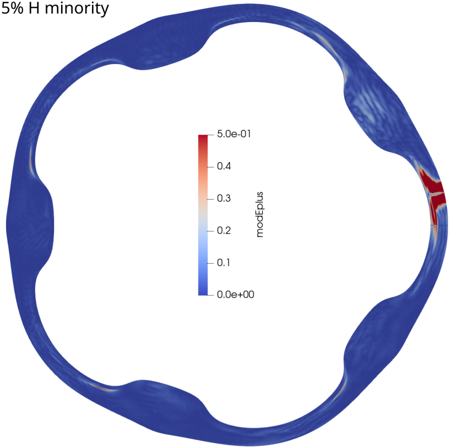

- overall shape of the wave field looks similar
- resonance only in the bean-shaped cross section and absent in triangular cross section
- depends on equilibrium (mirror ratio)

Comparison of the ICRH wave field ($|E_+|$)

10% H minority

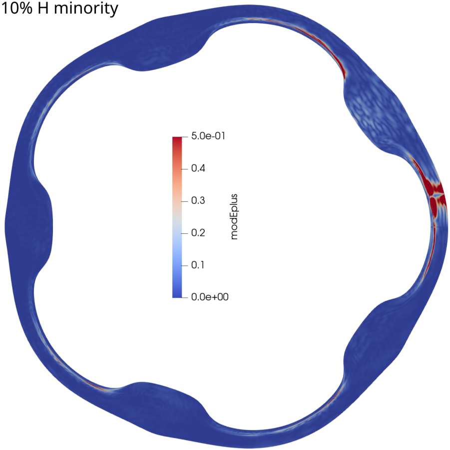

- overall shape of the wave field looks similar
- resonance only in the bean-shaped cross section and absent in triangular cross section
- depends on equilibrium (mirror ratio)

15% H minority

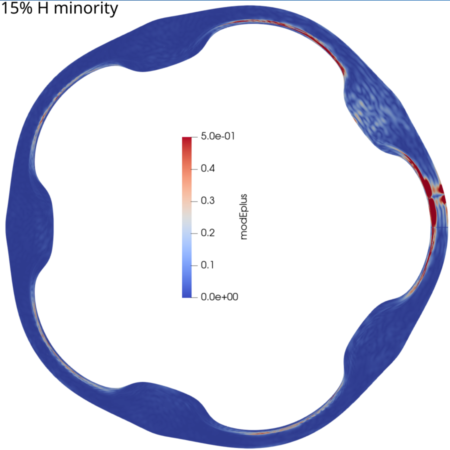

- overall shape of the wave field looks similar
- resonance only in the bean-shaped cross section and absent in triangular cross section
- depends on equilibrium (mirror ratio)

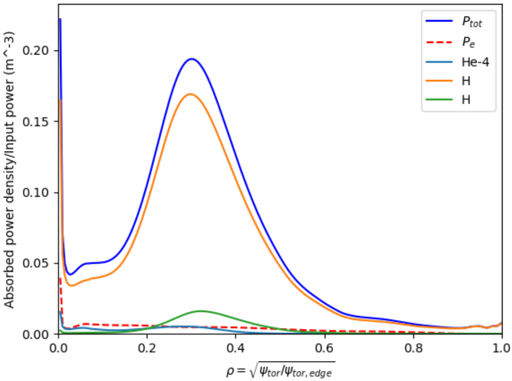

- as seen in previous results: no big difference between the two 5% and 10% cases
- much broader power deposition profile for 15% H minority
- large spike at $\rho = 0$ is artificial
- throughout these simulations it is assumed that $1\ \mathrm{MW}$ of power is coupled to the plasma

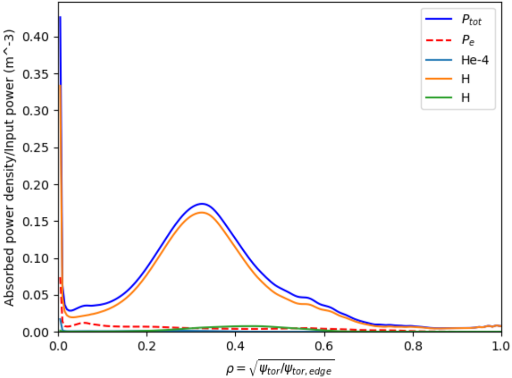

- as seen in previous results: no big difference between the two 5% and 10% cases
- much broader power deposition profile for 15% H minority
- large spike at $\rho = 0$ is artificial
- throughout these simulations it is assumed that $1\ \mathrm{MW}$ of power is coupled to the plasma

Comparison of the radial power deposition profiles

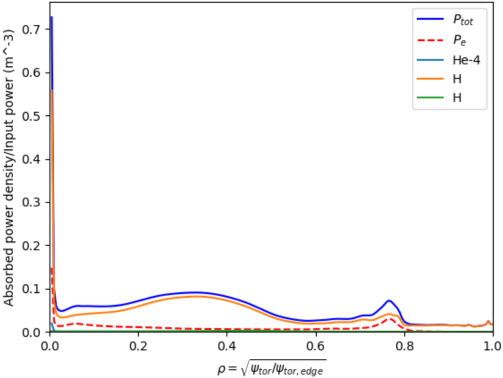

- as seen in previous results: no big difference between the two 5% and 10% cases
- much broader power deposition profile for 15% H minority
- large spike at $\rho = 0$ is artificial
- throughout these simulations it is assumed that $1\ \mathrm{MW}$ of power is coupled to the plasma

Next steps

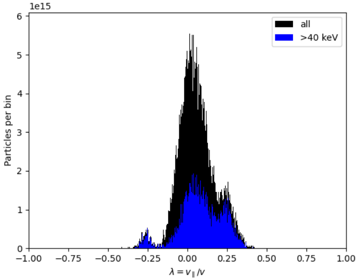

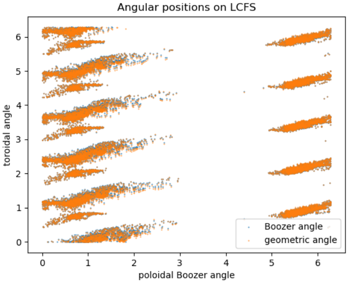

- data from particles lost in the VENUS-LEVIS simulation
- data for particle energy also available
- vary the bulk-plasma density: two more cases with $n = 1.0 \cdot 10^{20}\ \mathrm{m}^{-3}$ and $n = 1.5 \cdot 10^{20}\ \mathrm{m}^{-3}$ are running at the moment

- use lost-particle data for particle following in the SOL (ASCOT) to see where they hit the 3D wall / antenna
- find hot spots / compare to NBI / assess machine safety aspects

Interface to EUTERPE

- fast-ion distribution function computed by SCENIC is fitted to a modified bi-Maxwellian (analytical)

$$f_0 = \mathcal{N} \left(\frac{m}{2\pi T_\perp} \right)^{3/2} \exp \left[-m \left(\frac{\mu B_c}{T_\perp} + \frac{|E - \mu B_c|}{T_\parallel} \right) \right] \qquad (26)$$

- in practise, SCENIC provides radial profiles for $\mathcal{N}, T_\perp, T_\parallel$
- this distribution function is implemented in EUTERPE

- has been benchmarked successfully against the standard Maxwellian in the isotropic limit

⇒ stability analysis possible

- so far, the standard minority heating scheme (what was shown today) and the 3-ion scheme do not provide enough fast ions to affect the stability of AEs
- combined NBI/ICRH schemes will be investigated in the future

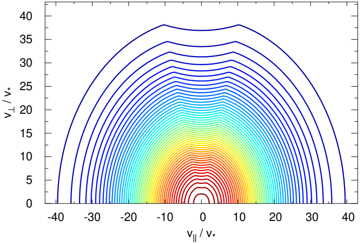

Summary and conclusions

CKA-EUTERPE:

- more general multi-mode version implemented (allows arbitrary phase factor for each mode)
- finite parallel electric field included

SCENIC:

- SCENIC code used to model ICRH physics in W7-X $\rightarrow$ preparation for upcoming campaign
- regular minority-heating scheme tried at different minority concentrations
- fast-particle losses to the wall/antenna will be assessed next
- distribution functions computed from SCENIC can be used in EUTERPE

Back-up slides